Nuclear Engineering and Technology 56 (2024) 3097–3111

Contents lists available at ScienceDirect

Nuclear Engineering and Technology

journal homepage: www.elsevier.com/locate/net

Original Article

Realistic estimation framework of radioactive release distributions into the environment during nuclear power plant accidents

Wasin Vechgama [a,b,c], Jaehyun Cho [d,*]

[a] Nuclear and Radiation Safety Division, Korea National University of Science and Technology, 217, Gajeong-ro, Yuseong-gu, Daejeon, Republic of Korea
[b] Korea Atomic Energy Research Institute, 111, Daedeok-daero 989 Beon-gil, Yuseong-gu, Daejeon, Republic of Korea
[c] Thailand Institute of Nuclear Technology (Public Organization), 16 Vibhavadi Rangsit Road, Chatuchak, Bangkok, Thailand
[d] Energy Systems Engineering, Chung-Ang University, 84 Heukseok-ro, Dongjak-gu, Seoul, Republic of Korea

ARTICLE INFO

Keywords:
Cesium-137
Severe accident risk
OPR-1000
Uncertainty analysis
Sensitivity analysis

ABSTRACT

Since the level 2 PSA of OPR-1000 was the requirement for regulatory purposes, Cs-137 release estimation was contained as the Nuclear Safety Act of ROK in which the Cs-137 release frequency exceeding 100 TBq was determined to happen less than 1.0E-6 per year after the Fukushima Daiichi Accident. However, Cs-137 release estimation from the conventional level 2 PSA of OPR-1000 provided uncertainty due to dominant accident sequence consideration. Thus, this study aimed to develop systematic methods through the overall framework to quantify realistic uncertainty concerns of radioactive material release using sensitivity and uncertainty analysis methods and apply them to OPR-1000. This framework helped to quantify confidential value for the Cs-137 release under the BEPU approach using both parametric and non-parametric methods to cover both realistic and conservative points. Uncertainty propagation analysis showed the unexpected uncertainty increase of Cs-137 release exceeding 100 TBq. The non-parametric uncertainty analysis provided higher conservative concerns for safety than the realistic concerns in terms of economics when compared with the parametric uncertainty analysis. Wilks' uncertainty analysis showed the importance to consider conservative Cs-137 release in order to reach the higher safety need. Sensitivity analysis showed reasonable relationships between engineering safety parameters with the Cs-137 release.

1. Introduction

In Nuclear Power Plants (NPPs), Probabilistic Safety Assessment (PSA) implementation is the essential process to improve their operational and financial performances, effectively and safely [1]. Risk assessment in PSA action aims to overcome the challenge of risky natural situations in order to change high-risky probability events to medium or low probabilities. Risk assessment of NPPs with complicated systematic processes was conducted to explain risk triplet questions including (1) What can go wrong? (2) How likely is it? and (3) What are the consequences? [2]. The risk triplet can lead to the understanding of outcomes, risk importance, and uncertainty. Since the complicated system from interfacing models in the PSA simulation generally happens uncertainty from any assumption, uncertainty analysis is an important tool to help determine acceptable risk performance [3]. In the same way, the Republic Of Korea (ROK) determines the PSA of NPPs as one of the requirements to confirm the safety of the plant for the decision-making process in any regulatory and commercial objectives [4]. Uncertainty analysis implementation of PSA is an important approach to providing reliable data on the PSA scheme.

In the ROK, Pressurized Water Reactor (PWR) is the most common-used reactor type in the industrial and household sectors especially the most use of Optimized Power Reactor-1000 (OPR-1000) [5]. The complicated full-scale of PSA Level 1, 2, and 3 PSAs of OPR-1000 were conducted to meet its safety criteria [6–11]. It was found that the full-scale PSA of three PSA levels required a lot of knowledge, processes, and models for covering the whole understanding of the accident sequences. Level 2 PSA is the important interface linking both the level 1 and level 3 PSAs [4]. Based on the Defense-in-Depth (DiD) [12], the containment vessel analysis in level 2 PSA was compared as the last main protection of source term release before moving to the environment. Specifically, the uncertainty of source term release in level 2 PSA receiving the input from level 1 PSA and transferring the output to level 3 PSA. Under the Nuclear Safety Act 2015 of the ROK, the Cs-137 release

* Corresponding author.
E-mail address: jcho@cau.ac.kr (J. Cho).

https://doi.org/10.1016/j.net.2024.03.009
Received 24 October 2023; Received in revised form 15 January 2024; Accepted 10 March 2024
Available online 22 March 2024

frequency exceeding 100 TBq was determined to happen not to be larger than 1 time in 1,000,000 reactor years (1.0E-6 per year) as in the voluntary target in Japan after the Fukushima Daiichi Accident [13].

Due to the importance of source term release of NPPs, there were many studies of uncertainty analysis covering the Cs-137 release in level 2 PSA from many countries. For example, in 2015, Japan studied the integrated approach to uncertainty and sensitivity analyses of nuclear reactor severe accident source terms of Unit 2 of the Fukushima Daiichi Nuclear Power Plant using integrated simulation code of THALES-2 and MELCOR [14]. Monte-Carlo-based uncertainty analysis was used to investigate the fractions of representative radionuclides of Cs-137 and cesium iodide (CsI). In 2021, China conducted the uncertainty analysis of radioactive source terms during a severe accident in level 2 PSA of Hualong Pressurized water Reactor-1000 (HPR-1000) using MAAP4 using Quantification and Uncertainty Analysis of Source Terms for Severe Accidents in Light Water Reactors (QUASAR) in 2021 [15]. The uncertainty data of Cs-137 source terms in level 2 PSA was calculated and transferred for providing the off-site dose rate in level 3 PSA using meteorology conditions in order to improve the emergency planning zone in case of no sheltering need beyond 3 km from HPR-1000. The ROK conducted the source term uncertainty evaluation using MELCOR in level 2 PSA of Westing House-600 (WH-600) to investigate off-site consequence uncertainty analysis using MACCS in level 3 PSA in early 2022 [16]. The Cs-137 and iodine-131 (I-131) were estimated and transferred to MACCS code for studying the effect of early health and late cancer. In a similar way, the level 2 PSA implementation of OPR-1000 of the ROK required the uncertainty analysis to estimate the confidential Cs-137 release using MAAP5 in order to confirm the acceptable source term risk consistently with the Nuclear Safety Act as mentioned before.

Conventional level 2 PSA of OPR-1000 was conducted to estimate the Cs-137 release from 19 Source Term Categories (STCs) by the final accumulated value of the Cs-137 release using MAAP5 code in the time function [9]. However, after the grouping process in level 1 PSA, the only dominant representative of level 1 PSA accident sequences would be transferred as the input of level 2 PSA for the conservative estimation. Consequently, the uncertainty of source term release output in level 2 PSA would increase unavoidably and possibly be able to affect the future level 3 PSA. Therefore, to provide more reliable data based on the Best Estimate Plus Uncertainty (BEPU), it is important to take into account the uncertainty analysis of overall Cs-137 consequences in the level 2 PSA for reflecting the issue of interactions between Deterministic Safety Assessment (DSA) and PSA for addressing and improving any design and operational issues and to serve the decision making in the regulatory area [17]. The objective of this study was to develop the overall realistic uncertainty analysis framework to quantify confidential points of radioactive materials release through Cs-137 release. This framework was applied to 19 STCs of the OPR-1000 case to quantify more reliable data for the confidential Cs-137 release. Also, the study investigated the sensitivity analysis to identify the major uncertainty parameters affecting the relationship Cs-137 consequence. Both parametric and non-parametric methods were used for uncertainty analysis and sensitivity analysis for understanding the data behavior in the framework.

This paper was divided into five sections. First, this section was the introduction section. The second section explained the uncertainty analysis framework. The third section provided the application of the uncertainty analysis framework in the OPR-1000 case study. The fourth section is the results and discussion of the uncertainty analysis and sensitivity analysis of the Cs-137 release in the OPR-1000 case study. The last section summarized the sensitive uncertainty parameter affecting the Cs-137 release and the suggestion on the proper use of uncertainty analysis methods for making a decision on aspects of safety and economy.

2. Uncertainty analysis framework

Fig. 1 shows the overall uncertainty analysis framework. The framework is designed to quantify realistic and conservative estimation of Cs-137 release of NPP accidents and understand the sensitive parameters affecting the uncertainty of the release. The conventional level 2 PSA, which provides only one representative Cs-137 release, is improved to estimate multiple Cs-137 releases using uncertainty parameter distributions based on the uncertainty analysis framework in Fig. 1 in order to estimate the confidential point of radioactive materials release. There were four main steps of the overall uncertainty analysis framework including (1) Nuclear accident scenario identification, (2) Uncertain parameter identification, (3) Radioactive materials release quantification, and (4) Metrics summary.

2.1. Step 1: Nuclear accident scenario identification

Representative accident scenario sequences from STCs based on the conventional PSA were determined for the case study.

2.2. Step 2: Uncertainty parameter identification

Uncertainty parameters were investigated and identified based on the MAAP5 developer in version 5.05 [18].

2.3. Step 3: Radioactive materials release quantification

Uncertainty input files per STC were generated based on uncertainty parameter distributions using Sampling Input and Quantifying Estimator (MOSAIQUE) for quantifying the Cs-137 release in the MAAP5 simulation.

2.4. Step 4: Metrics summary

Uncertainty and sensitivity analysis methods both parametric and non-parametric were applied to quantify the 95% confidential point and to identify the major uncertainty parameters affecting the relationship Cs-137 release. A parametric test was a specific assumption that population parameters behave underlying any distributions while a non-parametric test would not consider the assumption about population parameter distributions (considering only orders of parameters) [19].

3. Application of uncertainty analysis framework to OPR-1000 case study

3.1. Nuclear accident scenario identification

Table 1 shows the Cs-137 release of 19 STCs using the conventional level 2 PSA of OPR-1000 from MAAP5 simulation. In the nuclear accident identification step, all NPP accident scenarios were determined based on the risk model from the levels 1 and 2 PSA using conventional level 2 PSA implementation of OPR-1000. The representing accident scenarios of 19 STCs that were determined for this study were shown Table 1 without the consideration of uncertainty. In terms of the Cs-137 rule of the Nuclear Safety Act, STC1 and STC2 were considered accident scenarios releasing less than 100 TBq of Cs-137 with the assumption of a design leak rate of 0.1% volume per day without containment failure [10]. The remaining STCs were the accident scenarios releasing more than 100 TBq of Cs-137 with containment failure mode assumption in which the amount of release of each STC was dependent on their accident scenario types containment failure modes and safety feature operations such as the containment spray, debris cooling system, and so on.

3.2. Uncertainty parameter identification

Table 2 shows the uncertainty parameter and probability

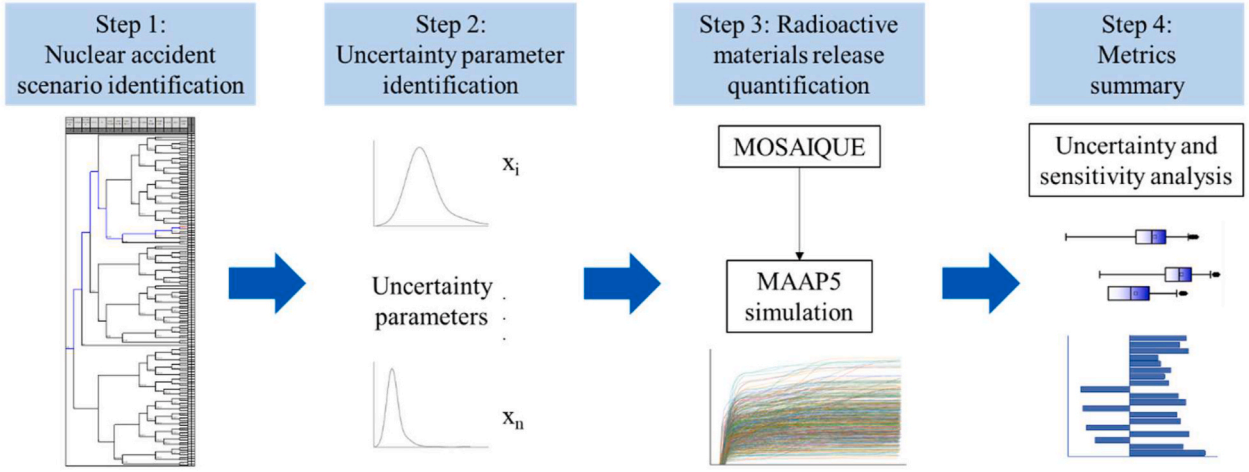

Fig. 1. Overall uncertainty analysis framework.

distribution information in the MAAP5 simulation based on engineering judgment. In this step, 58 uncertainty parameters and their distributions were investigated and identified based on the MAAP5 developers. These uncertainty parameters affecting the Cs-137 release during the accident progress were considered in MAAP5 version 5.05 [18] from the following phenomena consisting of in-vessel natural circulation, cladding rupture, core collapse, flow area at core collapse, zircaloy oxidation, in-vessel cooling, lower plenum debris cooling, fission product release, flow at the break area, engineered safeguard operation, and consideration of stating the time of accidents.

3.3. Radioactive materials release quantification

In this step, Cs-137 release was quantified to represent the radioactive materials release into the environment using MAAP5 simulation. The inputs for MAAP5 simulation were varied by uncertainty parameter distributions in Table 2 using the pre-processing process by MOSAIQUE code [20]. MOSAIQUE is software for uncertainty analysis to sample the parameters based on their distribution information and to generate sampling inputs for MAAP5 simulation using Monte Carlo. Each uncertainty parameter was set as the representative input to generate the uncertainty ranges based on their probability distribution types in Table 2.

In this study, the conventional level 2 PSA of OPR-1000 referred to only one representative simulation which is the base case for calculating the Cs-137 release in all 19 STCs as shown in Table 1. Instead, after considering the uncertainty parameter distributions around 610 simulations were developed for calculating the Cs-137 release for all 19 STCs. The reason for having 610 input files generated per one STC was that the work intended to study one of the scopes related to Wilks' method in five orders including a total of 610 cases per STC from Table 3. Thus, the number of 610 input files was set as the sample base for both parametric and non-parametric uncertainty analysis in this work. Table 3 shows the five-order classification of Wilks' method per one STC. The description and theory of Wilks' method will be shown in Subsection 3.4.1.3.

All input files were simulated using MAAP5 version 5.05 [18] using high-performance computers that time around 1–3 days per STC approximately depending on the required time of the simulation case. In this study, the first 610 simulation cases (original 610 MAAP5 simulation cases) of each STC were called the "representative case" for uncertainty analysis. Moreover, 610 simulation cases from the representative case of each STC were randomized at 10, 100, and 1000 times to provide the data set as in the five-order classification of Wilks' method in Table 3. Average values from the 10, 100, and 1000 times in randomized processes would be discussed to confirm the reasonability of uncertainty analysis methods as mentioned in Subsection 3.4.1.

3.4. Metrics summary

3.4.1. Uncertainty analysis

Uncertainty analysis was the important statistical analysis process in which parametric and non-parametric uncertainty analysis techniques were applied to calculate the 95% confidential point estimation from the uncertainty propagations of Cs-137 release in all 19 STCs in order to reflect the acceptable point that was adopted in the nuclear safety analysis [21]. The parametric uncertainty analysis method used the assumption based on the normal distribution of the population of the Cs-137 release in each STC for estimating the acceptable Cs-137 release at the 95% confidential point while the non-parametric uncertainty analysis applied the attribute of the population distribution without any assumption for estimating the 95% confidential point [19]. Both parametric and non-parametric uncertainty analysis techniques were applied to this work to consider the appropriate methods for the acceptable Cs-137 release in both realistic and conservative estimations. In this work, empirical analysis and goodness-of-fit test were studied as representative of parametric uncertainty analysis while Wilks' method was studied as representative of non-parametric uncertainty analysis.

3.4.1.1. Empirical analysis. The empirical analysis is the parametric statistical method applying the empirical rule of normal distributions to estimate the 95%/95% confidential estimation [19]. The normal distribution curve is considered a symmetric distribution, so the 95%/95% confidential estimation is approximated at the 95th percentile point in Eq. (1) as follows;

$$FoM_{s,95\%/95\%} = \mu_s + 1.645\sigma_s \tag{1}$$

where is the 95% confidential point estimation of samples, μ_s is the mean of samples, and σ_s is the standard deviation of samples.

3.4.1.2. Goodness-of-fit test. Goodness-of-fit test is the parametric statistical technique that is applied to estimate the 95% confidential point with the normal distribution assumption based on the 95% confidence level of the *t*-test and chi-square test [17]. If the normal distribution is assumed by the goodness-of-fit test, the population mean, and population standard deviation can be estimated based on the 95% confidence level based on the theories of the *t*-test and chi-square test. The final 95%/95% point estimation of goodness-of-fit test can be finally calculated by Eq. (2) as follows;

$$FoM_{p,95\%/95\%} = \mu_{p,95\%} + 1.645\sigma_{p,95\%} \tag{2}$$

where is the 95% confidential point estimation of the goodness-of-fit

Table 1
Cs-137 release of 19 STCs using the conventional level 2 PSA of OPR-1000 from MAAP5 simulation.

STC	Representing accident acenarios	Accident Scenario explanation	Containment failure mode	Description	Cs-137 release [TBq]*
1	SBOR38-CET3	Late station blackout in which diesel generators fail to run No. 38 - Containment event tree No. 3	No containment failure (Considering a design leak rate of 0.1% volume per day without containment failure)	Reactor vessel intact	1.59E-01[a]
2	SBOR38-CET4	Late station blackout in which diesel generators fail to run No. 38 - Containment event tree No. 4	No containment failure (Considering a design leak rate of 0.1% volume per day without containment failure)	Reactor vessel rupture	4.36E+00[a]
3	SBOR38-CET18	Late station blackout in which diesel generators fail to run No. 38 - Containment event tree No. 18	Early containment failure	Containment leak with containment spray on	4.17E-01[a]
4	TLOCCW04-CET20	Total loss of component cooling water No. 4 - Containment event tree No. 20	Early containment failure	Containment leak with containment spray off	1.34E+04[b]
5	SBOR38-CET22	Late station blackout in which diesel generators fail to run No. 38 - Containment event tree No. 22	Early containment failure	Containment rupture with containment spray on	3.89E+00[a]
6	TLOCCW04-CET24	Total loss of component cooling water No. 4 - Containment event tree No. 24	Early containment failure	Containment rupture with containment spray off	2.23E+04[b]
7	TLOCCW04-CET12	Total loss of component cooling water No. 4 - Containment event tree No. 12	Late containment failure	Containment leak with containment spray on	6.56E+03[b]
8	LOKVA12-CET53	Loss of 1E 4.16 kV AC BUS 02 M No. 12 - Containment event tree No. 53	Late containment failure	Containment leak with containment spray on and debris not cool	1.51E+00[a]
9	LODCA16-CET60	Loss of 1E DC BUS 01A No. 16 - Containment event tree No. 60	Late containment failure	Containment leak with Containment spray off and debris not cool	6.56E+03[b]
10	TLOCCW04-CET13	Total loss of component cooling water No. 4 - Containment event tree No. 13	Late containment failure	Containment rupture with containment spray off	8.31E+03[b]
11	LOKVA12-CET54	Loss of 1E 4.16 kV AC BUS 02 M No. 12 - Containment event tree No. 54	Late containment failure	Containment rupture with containment spray on and debris not cool	2.67E-01[a]
12	LODCA16-CET39	Loss of 1E DC BUS 01A No. 16 - Containment event tree No. 39	Late containment failure	Containment rupture with Containment spray off and debris not cool	9.41E+03[b]
13	LODCA16-CET59	Loss of 1E DC BUS 01A No. 16 - Containment event tree No. 59	Basement melt-through	Early reactor vessel rupture	4.09E+01[a]
14	LODCA16-CET70	Loss of 1E DC BUS 01A No. 16 - Containment event tree No. 70	In-vessel steam explosion	Early reactor vessel rupture	4.25E+04[b]
15	SLOCA2-CET98	Small loss of coolant accident No. 2 - Containment event tree No. 98	Containment failure before reactor vessel breach	Late reactor vessel rupture	1.86E+04[b]
16	LSSB-OUTCTMT-55-CET01	Large secondary steam line break (Outside the containment) No. 55 - Containment event tree No. 1	Non-containment isolation	Containment spray on	1.08E+03[b]
17	SBOR45-CET02	Late station blackout in which diesel generators fail to run No. 45 - Containment event tree No. 2	Non-containment isolation	Containment spray off	4.03E+03[b]
18	ISLOCA01-CET99	Interfacing system loss of coolant accident No. 1 - Containment event tree No. 99	Containment bypass	Interfacing system loss of coolant accident	2.64E+05[b]
19	SGTR13-CET100	Steam generator tube rupture No. 13 - Containment event tree No. 100	Containment bypass	Steam generator tube rupture	3.88E+04[b]

[a] Cs-137 release not exceeding 100 TBq
[b] Cs-137 release exceeding 100 TBq

test, $\mu_{p,95\%}$ is the population mean of the distribution on the 95% confidence level based on the theory of the *t*-test, and $\sigma_{p,95\%}$ is the population standard deviation of the distribution on the 95% confidence level based on the theory of the chi-square test.

3.4.1.3. Wilks' method. Fig. 2 shows the trend of the 95% confidential value of Wilks' theory in five orders. Wilks' method is the non-parametric statistical method applying the statistical tolerance limits with unknown distributions to calculate the 95% confidence point using the order of data. In this work, the one-sided statistical tolerance limits of Wilks' method [22] were applied to estimate the 95% confidence level based on all five orders in Fig. 2.

In principle, the higher order could represent a more realistic point while the lower order could represent a more conservative point. In this work, each order of Wilks' method with its number of simulation cases in Fig. 2 was used to represent the 95% confidence estimation point for the non-parametric uncertainty analysis method. For example, the 1st order means the maximum value among 59 simulation cases to represent the 95% confidence point. The 2nd order means the second largest value among 93 simulation cases to represent the 95% confidence point. The 3rd order means the third largest value among 124 simulation cases to represent the 95% confidence point. The 4th order means the fourth largest value among 153 simulation cases to represent the 95% confidence point. The 5th order means the fifth largest value among 181 simulation cases to represent the 95% confidence point.

3.4.2. Sensitivity analysis

Similarly, the parametric and non-parametric sensitivity analyses were referred to as the same principle of the parametric and non-parametric statistics of uncertainty analysis as mentioned in Subsection 3.4.1. In this work, the Pearson correlation coefficient was estimated to consider the relationship of uncertainty parameters in Table 2 with the Cs-137 release as representative of the parametric method while the Spearman correlation coefficient was used to consider the relationship of them as representative of non-parametric sensitivity analysis.

Table 2
Uncertainty parameter and distribution information in MAAP5 simulation based on engineering judgment [18].

Phenomena	Uncertainty parameter	Description	Min. value	Default value	Max. value	Distribution type
In-vessel natural circulation	FFRICX	Gas cross-flow friction coefficient [−]	0	0.25	1	Triangular
Cladding rupture	TCLMAX	Cladding rupture temperature [K]	100	2500	3000	Triangular
	TSPFAL	Core support plate failure temperature [K]	1000	1650	3113	Triangular
	FGPOOL	Geometric shape factor for in-core molten pool [−]	0.5	0.738	1	Triangular
Core collapse	LMCOL0	Collapse criteria parameter when no core node surrounding the particular core [−]	48	53	54	Triangular
	LMCOL1	Collapse criteria parameter for a core node below a collapsed core node [−]	48	53	54	Triangular
	LMCOL2	Collapse criteria parameter for a core node next to an empty core node [−]	48	53	54	Triangular
	LMCOL3	Collapse criteria parameter for a core node surrounded by empty core nodes [−]	48	53	54	Triangular
Flow area at core collapse	EPSCUT	Cutoff porosity below which the flow area and the hydraulic diameter of a core node are zero [−]	0	0.1	0.25	Triangular
	EPSCU2	Cutoff porosity below which the flow area and the hydraulic diameter of a collapsed core node are zero [−]	0.001	0.2	0.35	Triangular
	FGBYPA	Flag to divert gas flows in the core to the bypass channel when an entire axial row in the core is completely blocked [−]	0	1	1	Discrete
	FACT	Multiplier to reduce the hydraulic diameter and flow area when an intact fuel node collapses [−]	0.1	0.3	1	Triangular
	VFCRCO	Porosity of a collapsed core region [−]	0.05	0.35	0.5	Triangular
Zircaloy oxidation	FAOX	Multiplier for the cladding outside surface area [−]	1	1	2	Triangular
	FZORUP	Minimum fraction of Zr that must be oxidized to keep the cladding intact if the cladding is at cladding rupture temperature [−]	0	0.7	1	Triangular
	IOXIDE	Flag to select Zr oxidation model [−]	0	0	3	Discrete
In-vessel cooling	FQUEN	Multiplier to the flat plate critical heat flux for lower head debris bed quenching by overlying water [−]	0	0.2	1	Triangular
	ECREPF	Strain failure for vessel ductile material [−]	0	0.2	1	Triangular
	ECREPP	Maximum penetration weld strain at failure [−]	0.001	0.1	1	Triangular
	XGAP0	Initial size of the gap between the debris and the inner surface of penetrations in the lower head [m]	1.00E-06	1.00E-04	3.00E-04	Triangular
Lower plenum debris cooling	ENT0	Jet entrainment coefficient for the Ricou-Spalding correlation based on benchmarking against the latest KROTOS and FARO experiments [−]	0.025	0.045	0.06	Triangular
	IOCHF	Flag to choose the gap cooling CHF correlation [−]	0	0	2	Discrete
	IOXIDHT	Flag used by subroutine DBBED to choose the correlation for heat transfer from the oxidic corium pool to both the lower and the upper crust in the lower plenum [−]	0	0	2	Discrete
	HTCMCS	Nominal sideward heat transfer coefficient for convective heat transfer from molten corium to the side crust for corium-concrete interaction calculation [W/m^2.C]	500	3500	10000	Triangular
	HTCMCU	Nominal upward heat transfer coefficient for convective heat transfer from molten corium to the upper crust if the crust exists or upper interface if the crust does not exist for corium-concrete interaction calculation [W/m^2.C]	500	3500	10000	Triangular
	HTCMCR	Nominal downward heat transfer coefficient for convective heat transfer from molten corium to the lower crust for corium-concrete interaction calculation [W/m^2.C]	500	3500	10000	Triangular
	ENT0C	Jet entrainment coefficient for the Ricou-Spalding correlation for Level 2 sequences when there is a non-trivial amount of water in the pedestal or cavity when the vessel fails [−]	0.025	0.045	0.06	Triangular
	ENT0RB	Coefficient in Ricou-Spalding entrainment correlation for the off-gas entraining corium process [−]	0.025	0.08	0.1	Triangular
	HTFB	Coefficient for film boiling heat transfer from corium to an overlying pool [W/m^2.C]	100	300	400	Triangular
	IPBRB	Flag to control whether or not particle bed is formed on top of corium pool when corium jet is relocated from the vessel into the water pool in the reactor cavity [−]	0	0	1	Discrete
	IKCMOXIDE	Flag to use oxide thermal conductivity to calculate heat transfer rate from corium crust to water using Epstein's water ingression model [−]	0	0	1	Discrete
Fission product release	FPRAT	Value to represent testing model based on the results of benchmarking of in-core fission product release VI test series at ORNL [−]	−7	−6	7	Triangular
	FVPREV	Multiplier to the vapor pressures of CsI for revaporization calculations [−]	0.01	1	2	Triangular
	FCSIVP	Multiplier to the vapor pressures of CsI for vapor and aerosol equilibrium [−]	−100	1	100	Triangular
	FCSHVP	Multiplier to the vapor pressures of CsOH for both vapor and aerosol and vapor and surface equilibrium [−]	−100	1	100	Triangular
	FEFFDR	Aerosol capture efficiency of containment sprays [−]	0.01	0.02	0.05	Triangular
	FAERDC	Ratio of the existing airborne aerosol mass to the aerosol mass that would result in steady-state conditions [−]	1	8	100	Triangular
	GSHAPE	Gamma shape factor to account for non-spherical shapes in the aerosol coagulation calculations [−]	1	2.5	10	Triangular
	CSHAPE	Chi shape factor to account for non-spherical shapes of the aerosols in Stokes' Law for gravitational settling [−]	1	1	15	Triangular
	FE0	Aerosol collision efficiency [−]	0.33	0.33	1	Triangular
	XRDB	Radius of aerosol particles released from debris beds into overlying water pools [−]	1.00E-08	1.00E-08	1.00E-06	Triangular

(*continued on next page*)

Table 2 (*continued*)

Phenomena	Uncertainty parameter	Description	Min. value	Default value	Max. value	Distribution type
Flow at break area	AJUNC0(10)	Area of the junction 10 for rupture failure junction [m^2]	5.00E-02	1.00E-01	2.00E-01	Normal
	AJUNC0(9)	Area of the junction 9 for leak failure junction [m^2]	5.00E-03	1.00E-02	2.00E-02	Normal
	AJUNC0(8)	Area of the junction 8 for design leak junction [m^2]	7.00E-07	7.25E-06	7.00E-05	Normal
	ABBN(1)	Break area of the 1st break [m^2]	2.03E-03	8.10E-03	1.82E-02	Uniform
	ABBN(2)	Break area of the 2nd break [m^2]	1.27E-04	5.06E-04	2.02E-03	Probability Equation
	ASGTR(1)	Primary side loss of coolant accident break area for a steam generator tube rupture of the 1st break [m^2]	2.24E-04	4.48E-04	8.96E-04	Uniform
	AGO(1)	Flow area of the 1st generalized opening [m^2]	2.02E-03	1.82E-02	7.28E-02	Uniform
Engineered safeguard operation	NHPI	Number of operational high pressure injection pumps [−]	1	2	2	Discrete
	NLPI	Number of operational low pressure injection pumps [−]	1	2	2	Discrete
	NSPA	Number of operating spray pumps for the upper compartment sprays [−]	1	2	2	Discrete
	IMDAFW2ON	Flag to open motor driven auxiliary feedwater [−]	0	1	1	Discrete
	ITDAFW2ON	Flag to open turbine driven auxiliary feedwater [−]	0	1	1	Discrete
Stating time of accident	TIM4SBO	Time period before station backout [h]	1	2	4	Uniform
	TIM4TDP	Time period before stopped turbine driven pump due to battery depletion [h]	4	4	8	Uniform
	TIM4OSP	Time period before stopped operating spray [h]	4	6	8	Uniform
	TIM4ECF	Time period before early containment failure [h]	0.1	1	2	Uniform
	TIM4LCF	Time period before late containment failure [h]	2	4	6	Uniform

Table 3
Five-order classification of Wilks' method per one STC.

Wilks' method	1st order	2nd order	3rd order	4th order	5th order	Total
Number of simulation cases	59	93	124	153	181	610

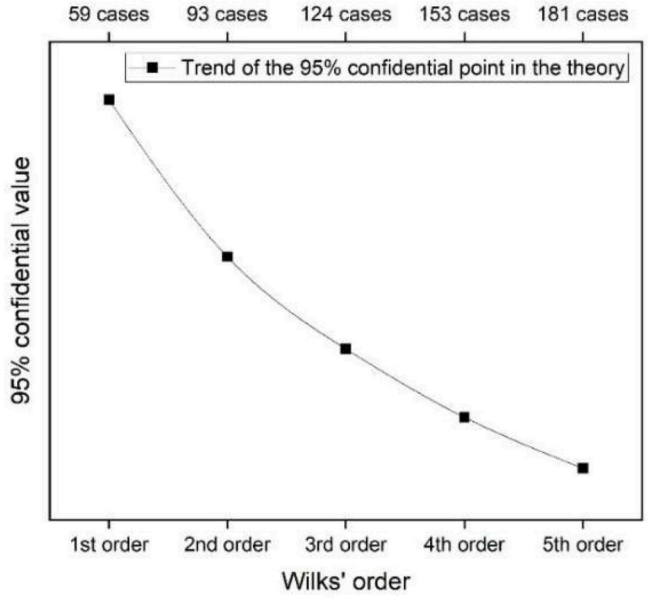

Fig. 2. Trend of the 95% confidential value of Wilks' theory in five orders.

3.4.2.1. Pearson correlation coefficient. Pearson correlation coefficient is the parametric sensitivity analysis method for measuring the linear relationship between two variables using the ratio of covariance of the two variables and the multiple of the standard deviation of each variable as shown in Eq. (3) [23,24]. Pearson correlation coefficient has a value between −1 and 1. If it is negative, two variables will have a negative linear relationship. On the other hand, its positive value will represent a positive linear relationship. Its zero value means no linear relationship between the two variables.

$$r_P = \frac{\sigma(x,y)^2}{\sigma(x)\sigma(y)} \tag{3}$$

where r_P is the Pearson correlation coefficient, $\sigma(x,y)^2$ is the covariance of variables x and y, $\sigma(x)$ is the standard deviation of variables x, and $\sigma(y)$ is the standard deviation of variables y.

3.4.2.2. Spearman correlation coefficient. Spearman correlation coefficient is the non-parametric sensitivity analysis method for measuring the relationship between two variables that can be described as a monotonic function using the relationship of the same order rank of the two variables as shown in Eq. (4) [25,26]. The Spearman correlation coefficient has a value between −1 and 1. If it is negative, two variables will have a negative monotonic relationship. On the other hand, its positive value will represent a positive monotonic relationship. Its zero value means no monotonic relationship between the two variables.

$$r_S = 1 - \frac{6\sum d^2}{n(n^2-1)} \tag{4}$$

where r_S is the Spearman correlation coefficient, d is the rank difference between the two variables, and n is the number of ordered pairs.

4. Results and discussion of OPR-1000 case study

This section provided the results and discussion of the application of the uncertainty framework to quantify the confidential point of radioactive materials characteristics of OPR-1000 accident scenarios from 19 STCs. The Cs-137 release results, the 95% confidential point estimations from the uncertainty analysis, and sensitive parameters were discussed below.

4.1. Uncertainty propagation analysis

Fig. 3 shows the uncertainty propagation of the Cs-137 release of 19 STCs. Hereafter all STCs in the paper would refer to the accident scenario name in Table 1. For calculating the Cs-137 release of all 19 STCs, the 19 MAAP5 inputs of 19 STCs from the conventional level 2 PSA of OPR-1000 from Table 1 were sampled the uncertainty parameters based

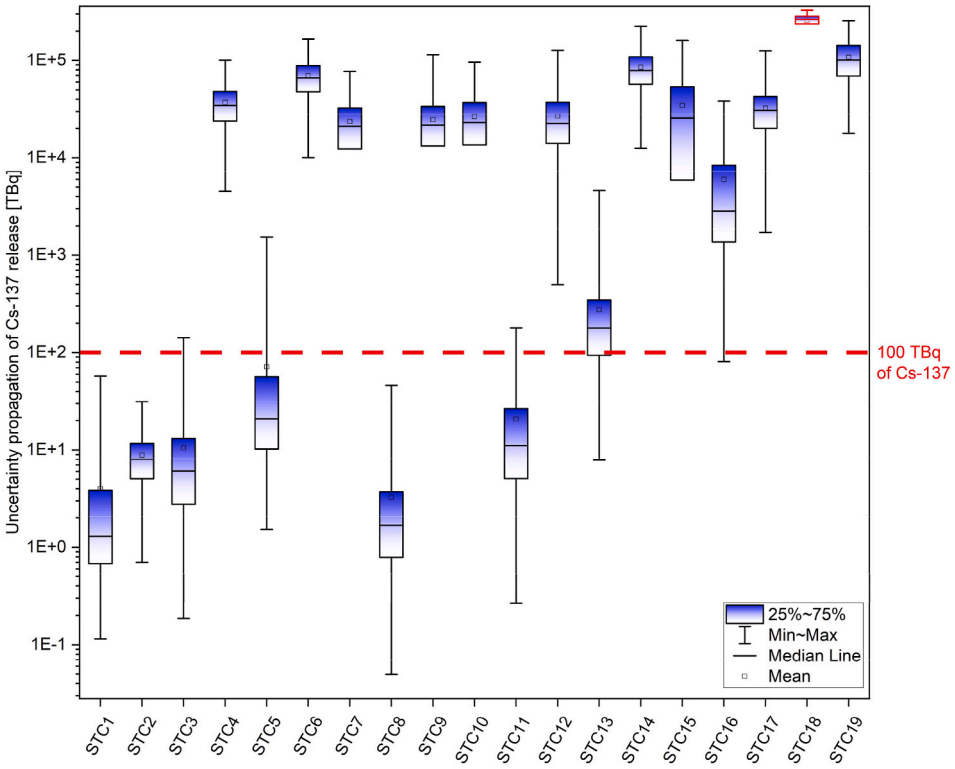

Fig. 3. Uncertainty propagation of Cs-137 release of 19 STCs.
(Hereafter all STCs in the paper would refer to the accident scenario name in Table 1).

on their probability distributions from Table 2 using MOSAIQUE and to generate 610 MAAP5 input files per one STC to calculate Cs-137 release of all 19 STCs. As a result, the Cs-137 release of 610 cases of all 19 STCs was shown as uncertainty propagation form in Fig. 3. It was found that the Cs-137 release average values of STCs including STC1, STC2, STC3, STC5, STC8, and STC11 were recognized as the Cs-137 release not exceeding 100 TBq. As the accident description in Table 1, STC1 and STC2 happened without the containment failure, thus the small Cs-137 release effect was mainly caused by the default design leak estimation. Although STC3, STC5, STC8, and STC11 happened with containment failure, it seemed like the safety features such as containment spray in the system could affect the prohibition of the Cs-137 release well. The uncertainty parameters and their related features affecting the Cs-137 release of each STCs would be discussed in detail in the sensitivity analysis in Section 4.3. Moreover, STC3, STC5, and STC11 were able to provide the uncertainty propagation of Cs-137 release exceeding 100 TBq from which they represented the chance of higher consequences that have to concern more.

Fig. 4, Fig. 5, and Fig. 6 show the uncertainty propagation of Cs-137 release of STC3, STC5, and STC11, respectively. The uncertainty propagations of Cs-137 release of STC3 in Fig. 4, STC5 in Fig. 5, and STC11 in Fig. 6 were plotted to show the examples of the extension of uncertainty range higher than 100 TBq. If considering the standard of Cs-137 release at 100 TBq from the Nuclear Safety Act in 2015 of ROK, it was found that these three cases provided the increase of the Cs-137 release more than 10 times of 100 TBq significantly when compared with the medium line of their box plots. Thus, STC3, STC5, and STC11 reflected the need for reconsideration with uncertainty concerns to determine Cs-137 release in the conservative case with the highest Cs-137 consequences consistently with the risk safety goal at the exceeding 100 TBq of Cs-137 release of their Cs-137 release.

Fig. 7, Fig. 8, Fig. 9, and Fig. 10 show the uncertainty propagation of Cs-137 release of STC4, STC6, STC13, and STC16. On the other hand, in Fig. 3, most of the STCs, having high average and middle points of Cs-

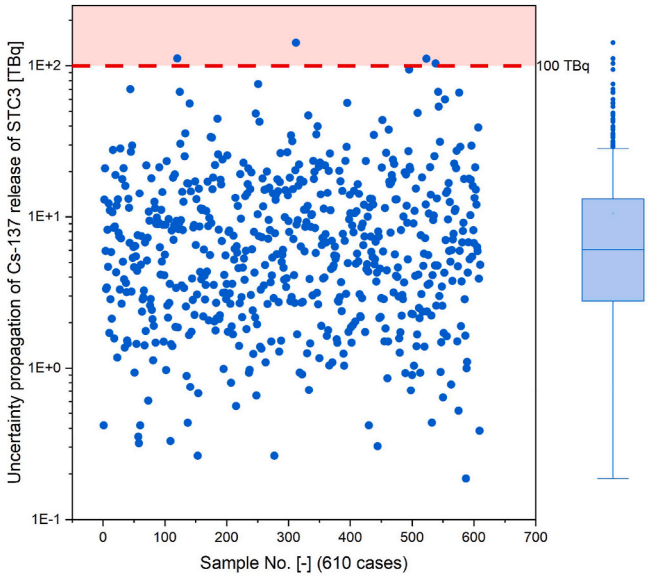

Fig. 4. Uncertainty propagation of Cs-137 release of STC3.

137 release exceeding 100 TBq, including STC4, STC6, STC7, STC9, STC10, STC12, STC13 STC14, STC15, STC17, STC18, and STC19, would have no extension of the uncertainty range of Cs-137 release lower than 100 TBq. The uncertainty propagation of maximum Cs-137 release of STC4 in Fig. 7, and STC6 in Fig. 8, were plotted to show the examples of the no extension of uncertainty range of Cs-137 release lower than 100 TBq. There were only STC13, and STC16 providing the extension of the uncertainty range lower than 100 TBq as shown in Figs. 9 and 10 respectively. It was found there were some data from the first quartile of 610 cases of STC13, and STC16 providing the extension of the

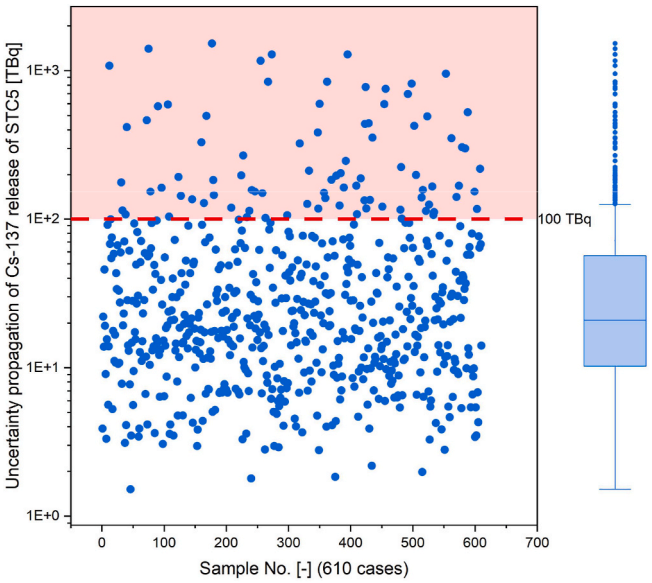

Fig. 5. Uncertainty propagation of Cs-137 release of STC5.

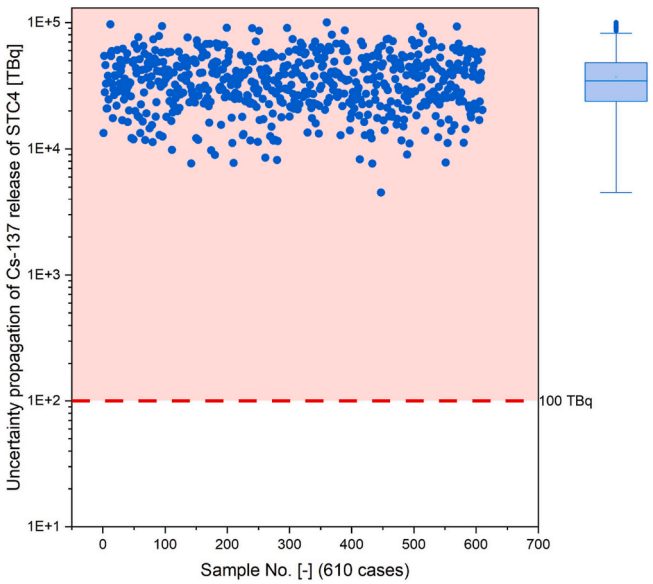

Fig. 7. Uncertainty propagation of Cs-137 release of STC4.

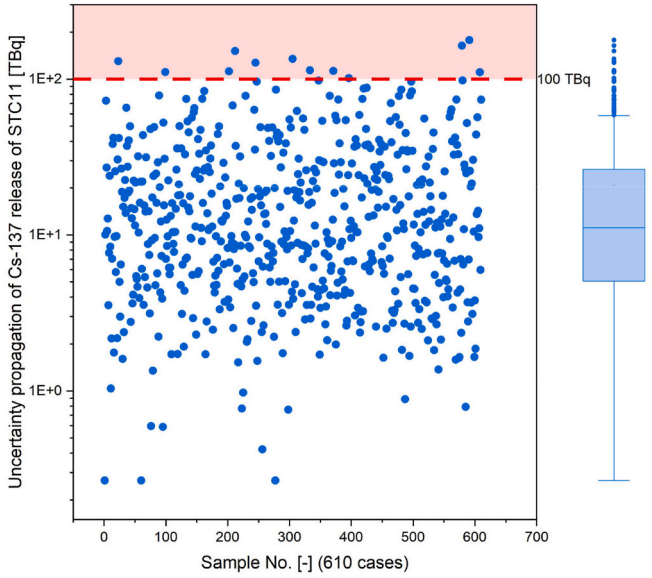

Fig. 6. Uncertainty propagation of Cs-137 release of STC11.

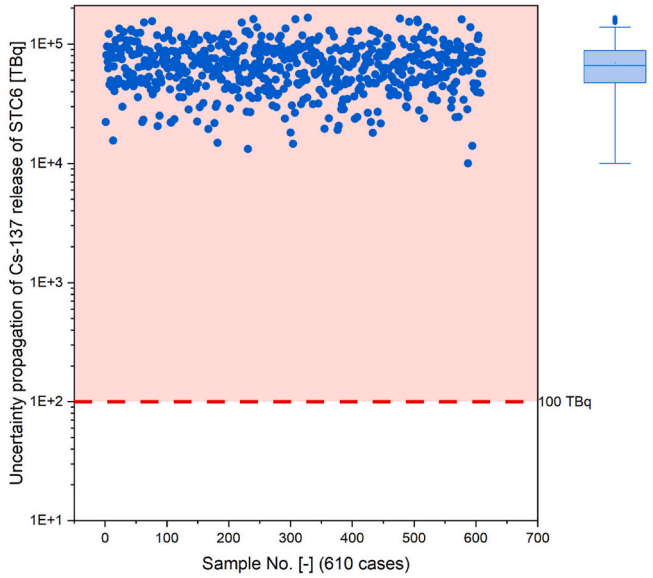

Fig. 8. Uncertainty propagation of Cs-137 release of STC6.

uncertainty range lower than 100 TBq. Although STC13 and STC16 provided the uncertainty range of Cs-137 release lower than 100 TBq inconsistently other STCs having very high Cs-137 release and exceeding 100 TBq, the majority of data cases still kept the uncertainty range of Cs-137 release higher than 100 TBq representing the characteristic of the high Cs-137 consequences dominantly.

Therefore, when comparing all STCs having the extension of uncertainty range higher and lower than 100 TBq in overall from the discussion above, it was confirmed that the determination of the Cs-137 release frequency exceeding 100 TBq for the regulatory purpose could be mainly affected by the STCs having the extension of uncertainty range of Cs-137 release higher 100 TBq i.e., STC3, STC5, and STC11. Moreover, the uncertainty propagation of Cs-137 release of 16 STCs in a total of 19 STCs provided the highest Cs-137 consequences higher than 100 TBq in the conservative consideration. Thereby, it is important to apply statistical analysis techniques of uncertainty analysis to justify the reliable data in realistic and conservative concerns to represent the proper uncertainty of Cs-137 release to serve both the safety and economic aspects of nuclear regulatory bodies and industries. Statistical uncertainty analysis was discussed in Subsection 4.2. Additionally, to investigate uncertainty parameters affecting the extension of the uncertainty range of the Cs-137 release in all 19 STCs, the sensitivity analysis was discussed in Subsection 4.3.

4.2. *Parametric and non-parametric uncertainty analysis*

Fig. 11 shows the 95% confidential point estimation of the Cs-137 release using the parametric uncertainty analysis of 19 STCs. Firstly, the parametric uncertainty analysis consisting of empirical analysis and the goodness-of-fit test was implemented to estimate the acceptable value at the 95% confidential point as shown in Fig. 11. It was found that all 19 STCs of the parametric uncertainty analysis provided consistent results whereby the 95% confidential points of empirical analysis had higher values than that of goodness-of-fit test method harmonizingly their theories [17,21]. According to the theories from Eq. (1) and Eq. (2), the 95% confidential point empirical analysis calculated by the mean of

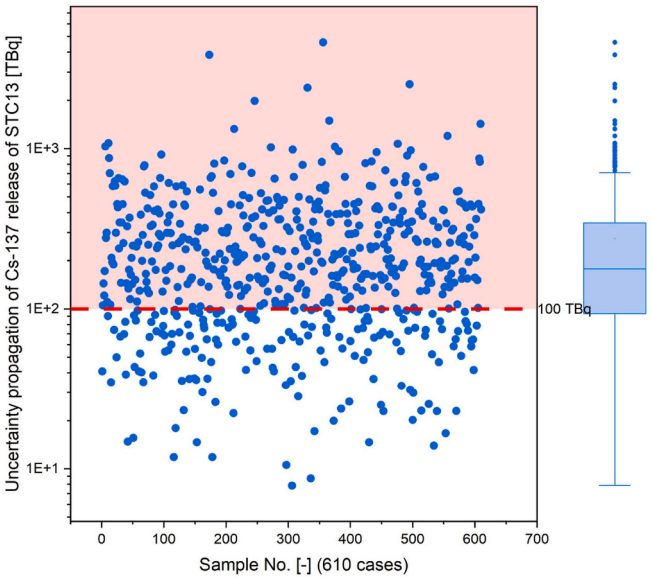

Fig. 9. Uncertainty propagation of Cs-137 release of STC13.

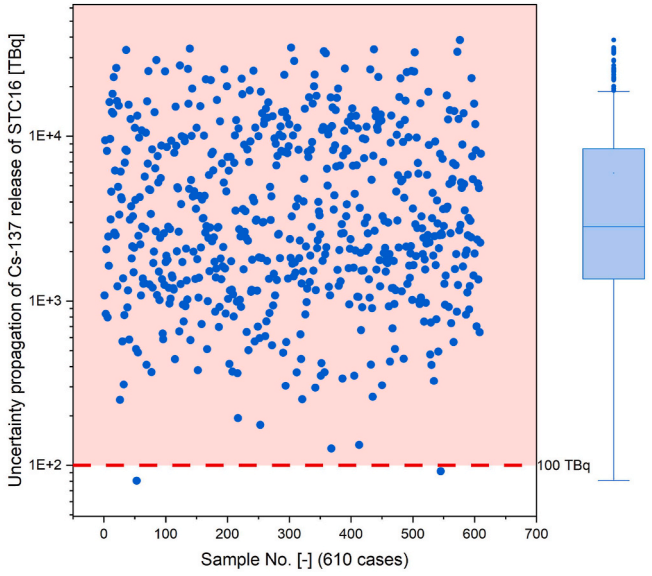

Fig. 10. Uncertainty propagation of Cs-137 release of STC16.

the distribution, and standard deviation always provided a wider range of consideration for the 95% confidential point of normal distribution assumption when comparing with the goodness-of-fit test method. In the goodness-of-fit test estimation, the effect of the 95% confidential point of the population means using the *t*-test and the 95% confidential point of population standard deviations from the chi-square test helped represent the estimation of the populations of generated normal distribution more properly and realistically.

Fig. 12 shows the conservatism comparison between the parametric uncertainty analysis methods of empirical analysis and the goodness-of-fit test at 95% confidential point of Cs-137 release of all 19 STCs. As discussed previously, when comparing the two parametric uncertainty analyses, the 95% confidential point of the goodness-of-fit test had the potential to represent the highest realistic point for the parametric method while that of empirical analysis could be recognized as the highest conservative point for the parametric method. Thus, the difference between the 95% confidential point of Cs-137 release of empirical analysis and the goodness-of-fit test was calculated to find the conservatism increase when using the goodness-of-fit test as the realisticism baseline. It was found that the conservatism increases of Cs-137 release in all 19 STCs when using empirical analysis were around 0.08%–0.34% when compared with the goodness-of-fit test. Although the conservatism comparison of empirical analysis slightly increased when compared with the goodness-of-fit test, these values would be important when the conservatism increase data were compared as the indicator for considering the uncertainty data in safety and economic aspects. In safety aspects, in this case, the use of the parametric uncertainty method of empirical analysis for making a decision, the highest conservative point helped confirm more confidential safety at 0.08%–0.34% for all 19 STCs cases but the cost for designing or improving the measurement and system would more increase as well. In contrast, the use of the parametric uncertainty method of the goodness-of-fit test provided less cost for considering the measurement and system improvement with lower confidential safety.

Fig. 13 shows the 95% confidential point from Wilks' method in five orders from the representative case. Regarding the result of Wilk's method of the representative case in Fig. 13, it was found that only one representative case (610 outputs), such as STC5 (◆) and STC13 (×) in the middle of the graph, was not precise enough to represent the proper 95% confidential point for the non-parametric method. This was because the results from Wilks' method from the representative case in five orders fluctuated and were not consistent with the theory that the 95% confidential points of Wilk's method would decrease when the orders of Wilk's method increased as shown in Fig. 2 [22]. Thus, it is essential to consider more data sets of simulation cases from the randomness analysis to confirm the reasonability of the non-parametric uncertainty analysis of Wilk's method. The randomness analysis proceeded by randomizing Cs-137 release from 610 simulation cases based on the numbers of Wilk's method suggested in each order in Fig. 2 using a simple randomness function in Microsoft Excel or Python code.

Fig. 14, Fig. 15, and Fig. 16 show the average value of the 95% confidential point of Wilks' method in five orders from the randomness cases at 10 times, randomness cases at 100 times, and randomness cases at 1000 times, respectively. 610 simulation cases from the representative case of all 19 STCs were randomized at 10, 100, and 1000 times to consider the proper uncertainty data for the non-parametric uncertainty analysis of Wilk's method. It was found that the average values at the 95% confidential points of the randomness at 10, 100, and 1000 times of Wilk's method cases in Figs. 14, Fig. 15, and Fig. 16 were more consistent with the theory when the number of randomness cases increased significantly. Especially, at the high randomness of Wilk's method of 100 times in Figs. 15, and 1000 times in Fig. 16, the 95% confidential points of Cs-137 release would convert to the stable value consistently with Wilk's method theory. Thus, the 95% confidential point from the randomness from 100 times to 1000 times was proper to explain as the characteristic of the non-parametric uncertainty analysis of Wilk's method due to the consistency of the theory. When considering the average value of the 95% confidential point from Wilks' method from the randomness cases in the 1st order, 2nd order, 3rd order, 4th order, and 5th order, it was found that the amount of 95% confidential points of Cs-137 release would decrease when Wilks' order increased according to the theory [22]. This meant that in the non-parametric estimation of this work, basically, 95% confidential point of Cs-137 release from the 1st order of Wilks' method could represent the highest conservative case supporting safety regulation issues well, while 95% confidential point from the 5th order of Wilks' method would be able to express the realistic estimation severing economic concerns.

Fig. 17 shows the conservatism comparison of 95% confidential point of Cs-137 release between the 5th order of Wilks' method from the randomness cases at 1000 times and the goodness-of-fit test. As discussed in Fig. 12, the goodness-of-fit test had the potential parametric method to represent the highest realistic point for the 95% confidential point of Cs-137 release. In order to compare the difference between parametric and non-parametric uncertainty analysis methods, the 5th

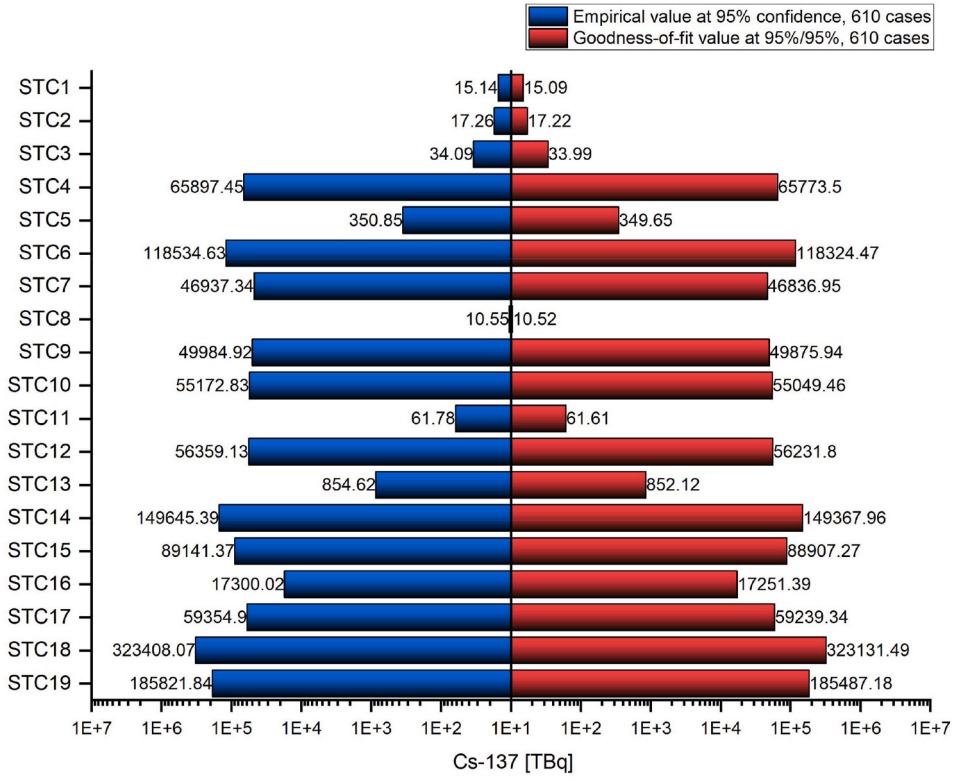

Fig. 11. 95% confidential point of Cs-137 release using empirical analysis and the goodness-of-fit test.

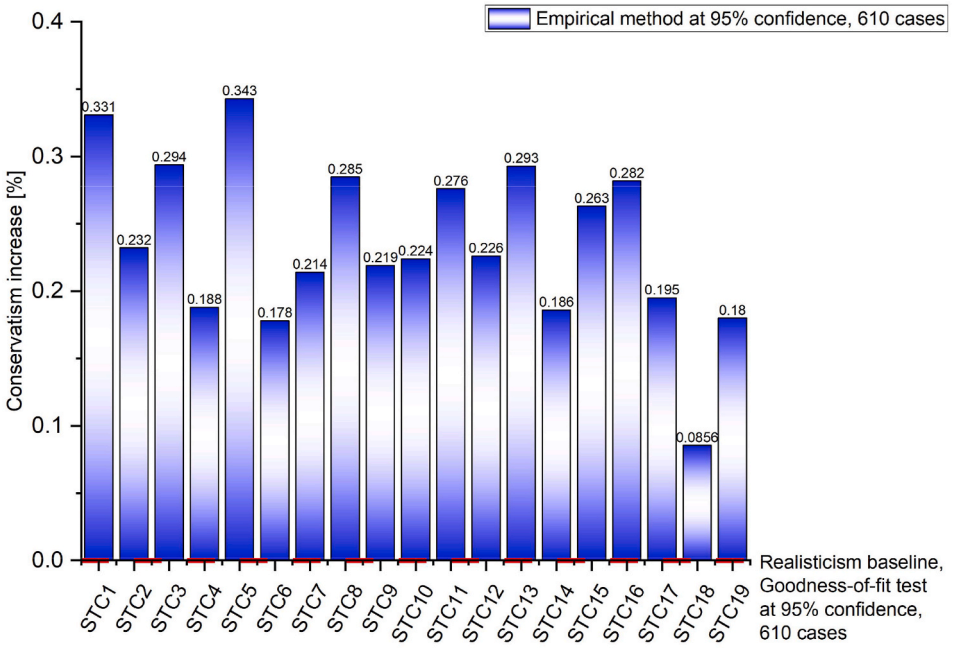

Fig. 12. Conservatism comparison of 95% confidential point of Cs-137 release between empirical analysis and the goodness-of-fit test. (Ratio of the results from empirical analysis to the results goodness-of-fit test).

order of Wilks' method from the randomness cases at 1000 times, representing the realistic estimation with the lowest order for the non-parametric uncertainty method shown in Fig. 16, was used to compare with the parametric uncertainty method of the goodness-of-fit test to discuss the conservatism aspects of them as shown in Fig. 17. It was found that although the 95% confidential point of Cs-137 release of 5th order of Wilks' method represented the lowest values for parametric method, most of the STCs from 5th order of Wilks' method significantly provide higher conservatism than the parametric uncertainty method of the goodness-of-fit test around 11.6%–71% depending on their data distribution of each STC. Conservatism would also increase when the order of Wilks' method decreased due to the higher values of 95% confidential points according to the theory [22]. Thus, in general, the most use of the non-parametric uncertainty analysis of Wilks' method

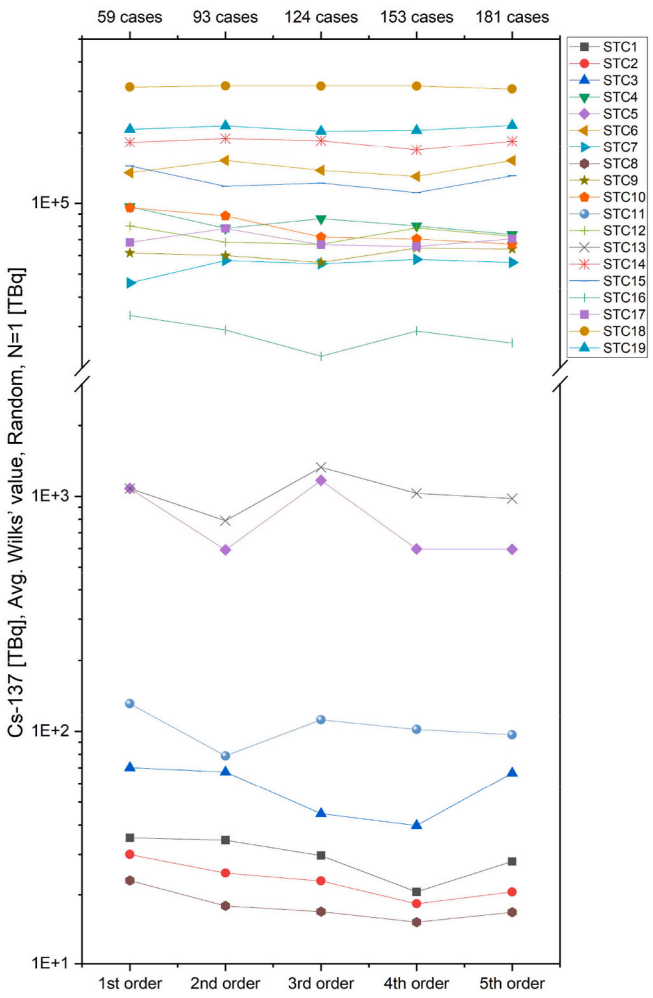

Fig. 13. 95% confidential point from Wilks' method in five orders from the representative case.

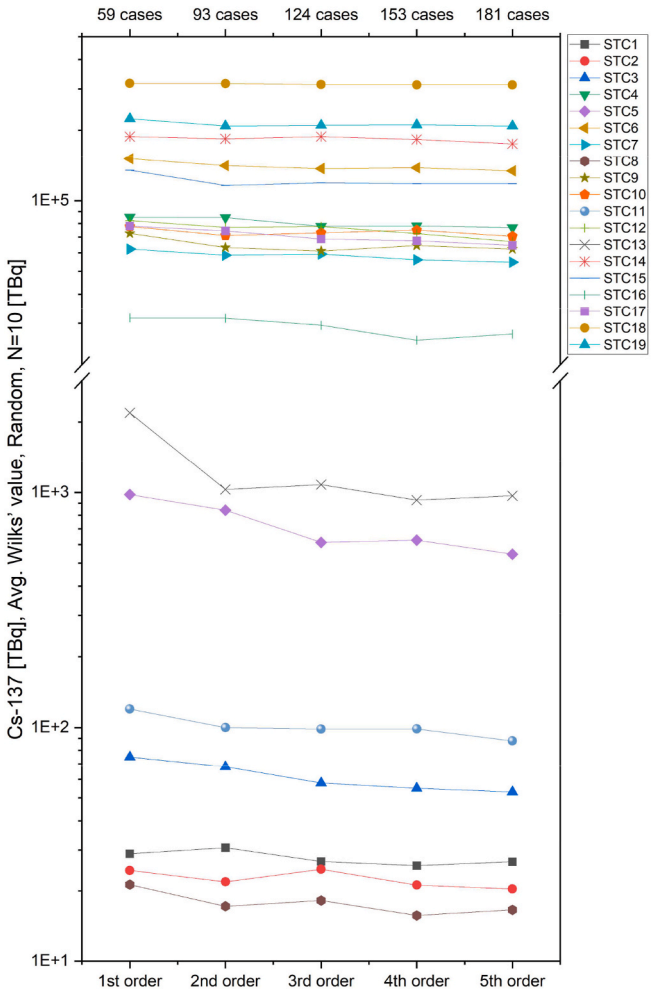

Fig. 14. 95% confidential point from Wilks' method in five orders from the randomness cases at 10 times.

provided higher conservative concerns for safety than the economic concerns for making a decision when compared with the parametric uncertainty analysis of the goodness-of-fit test.

Figs. 18 and 19 show the uncertainty bands of the Cs-137 release and the uncertainty distribution of the maximum Cs-137 release of STC18, respectively. However, from Fig. 17, the only STC18 case represented that the non-parametric uncertainty analysis of Wilks' method provided lower conservative concerns when compared with the parametric uncertainty analysis of the goodness-of-fit test. The uncertainty bands and the uncertainty propagation of maximum Cs-137 release of STC18 were used to investigate this phenomenon. As shown in the uncertainty propagation of maximum Cs-137 release of all 19 STCs in Fig. 3, it was found that there was only the STC18 case provided the narrow uncertainty distribution at the highest Cs-137 release range when compared with other STCs. The uncertainty bands of the Cs-137 release of STC18 in Fig. 18 showed the unique even uncertainty distributions having a narrow area base of almost data at the high Cs-137 release range. Due to the narrow uncertainty distribution of almost data in the high range, the approximation of 95% confidential point estimation using the theory of goodness-of-fit test in Eq. (2) using 95% confidential level of the population mean and standard deviation, was close to the maximum value of the uncertainty distribution as shown in Fig. 19. Thus, it was possible that the parametric uncertainty analysis of the goodness-of-fit test provided more conservative concerns than of the non-parametric uncertainty analysis of Wilks' method, especially in the narrow even uncertainty distributions at the high Cs-137 release range as in the STC18 case.

4.3. Parametric and non-parametric sensitivity analysis

Figs. 20 and 21 show the 1st rank of uncertainty parameters affecting the Cs-137 release of all 19 STCs using the Pearson correlation coefficient and the Spearman correlation coefficient, respectively. Hereafter uncertainty parameters would refer to the phenomena in Table 2. Due to the extension of the uncertainty range affecting the determination of the Cs-137 release frequency exceeding 100 TBq for the regulatory body as discussed in Subsection 4.1 and Subsection 4.2, the sensitivity analysis of 58 uncertainty parameters in MAAP5 from Table 2 was conducted to investigate the relationship of uncertainty parameters with the Cs-137 release using Pearson correlation coefficient as parametric sensitivity analysis and Spearman correlation coefficient as non-parametric sensitivity analysis. From Figs. 20 and 21, it was found that when comparing sensitivity analysis methods of the Pearson correlation coefficient and Spearman correlation coefficient, most of the 1st rank uncertainty parameters from 15 STCs had a consistent relationship between the two methods. Although, some STCs such as STC1, STC3, STC5, STC15, and STC16 provided different uncertainty parameters affecting the Cs-137 release from the two methods, the relationship of the different uncertainty parameters with the Cs-137 release from the two methods was reasonable because these uncertainty parameters were related to the physical characteristics of source terms release, and break area and engineering safety features affecting the source terms release. There

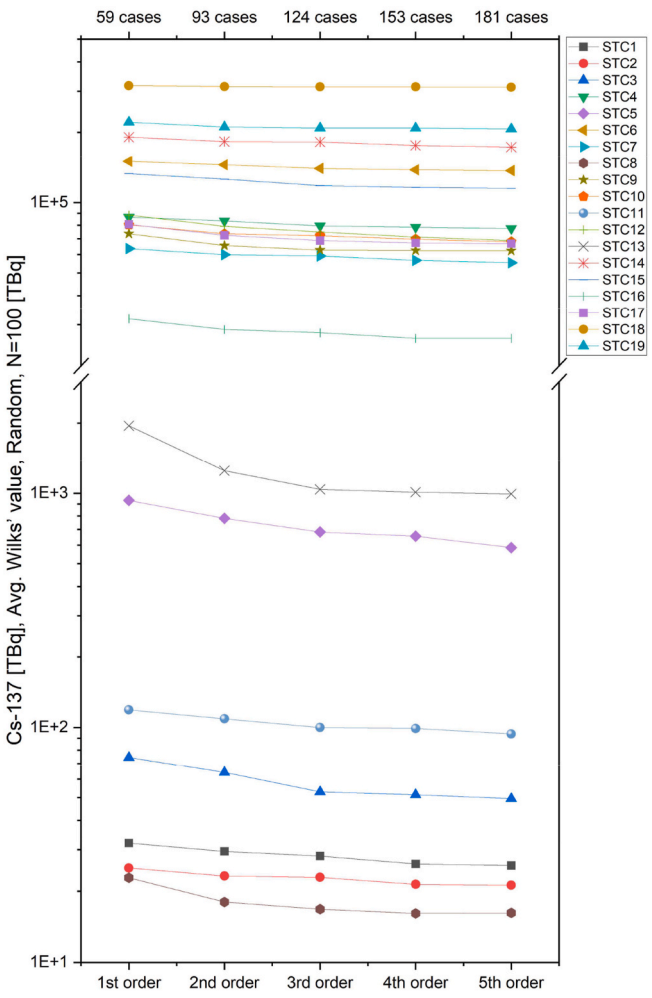

Fig. 15. 95% confidential point from Wilks' method in five orders from the randomness cases at 100 times.

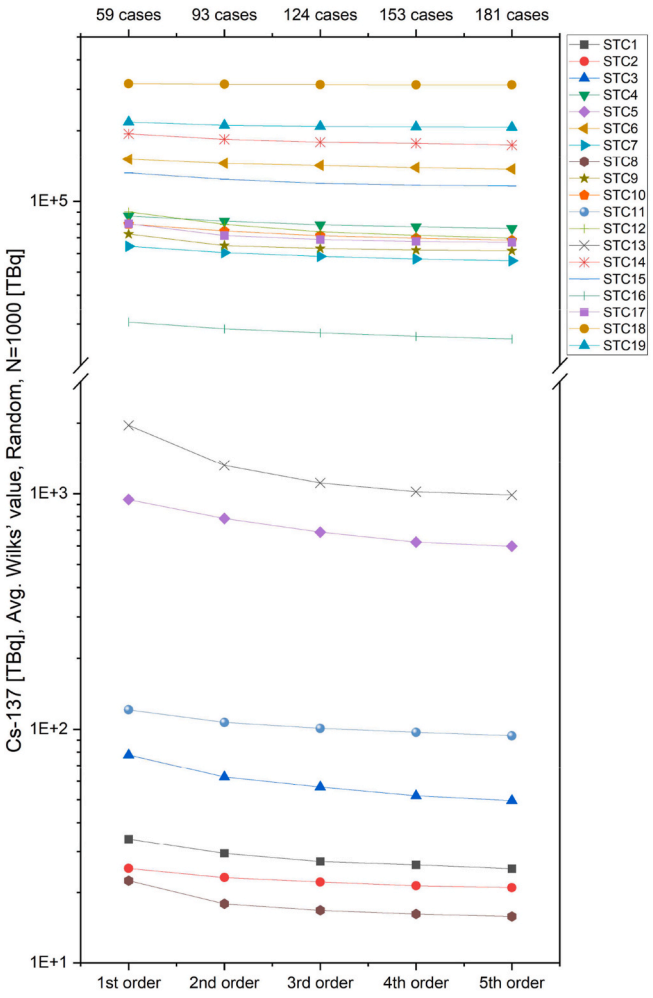

Fig. 16. 95% confidential point from Wilks' method in five orders from the randomness cases at 1000 times.

were seven dominant uncertainty parameters including ABBN(1): 1st break area in the primary system, ABBN(2): 2nd break area in the primary system, ASGTR(1): 1st break area of steam generator tube, CSHAPE: Chi shape factor for non-spherical shapes of the aerosols, NLPI: Number of operational low-pressure injection pumps, NSPA: Number of operating spray pumps for the upper part, and TIM4ECF: Time period before early containment failure, affecting the Cs-137 release of all 19 STCs using Pearson correlation coefficient and Spearman correlation coefficient.

First, 1st break area in the primary system, and 2nd break area in the primary system were the parameters the to determine break size of the Loss Of Coolant Accident (LOCA) dependent on the specific areas in the primary coolant system. Especially, in small LOCA in STC15, break area size in the primary coolant system became the major uncertainty parameter affecting the Cs-137 release. Second, 1st break area of the steam generator tube was the LOCA break area for a Steam Generator Tube Rupture (SGTR) event directly affecting the Cs-137 release, especially in STC19 occurring the containment bypass due to SGTR. Then, Chi shape factor to account for non-spherical shapes of the aerosols in Stokes' Law for gravitational settling [27] represented the deposition behavior of aggregates with variable aerosol sizes in which the increase of the shape factor contributed to the more compact aerosols affecting the easier release during both early and late containment failure cases such as STC6 and STC7, respectively. Next, the number of operational low-pressure injection pumps and the number of operating spray pumps for the upper part were used to the engineering safety feature input parameters to mitigate the Cs-137 release. For example, in late containment leak and rupture with containment spray on with debris not cooling in STC8 and STC11, respectively, these two parameters behaved as the major safety feature preventing the Cs-137 release. Finally, time period before early containment failure was the important parameter input for determining the time of Cs-137 release during the accident. Especially, the early containment failure cases due to Station Black-Out (SBO) such as STC3 and STC5 cases would be sensitive to the starting time of containment failure depending on the factor of AC power timeline from outside.

5. Conclusions

Since the full-scale PSA of OPR-1000 was required to implement based on regulatory and commercial purposes. Level 2 PSA, which was the interface linking between the level 1 and level 3 PSAs, became the important node that had the potential to receive and release the uncertainty data of other PSA levels. One of the uncertain data, that was recognized, was the Cs-137 release as contained as the safety standard in the Nuclear Safety Act of ROK in which the Cs-137 release frequency exceeding 100 TBq was determined to happen not to be larger than 1.0E-6 per year. This study aimed to develop the uncertainty framework to quantify the confidential point of radioactive materials release and apply it to OPR-1000 through the implementation of uncertainty analysis of the level 2 PSA of OPR-1000 case study of all 19 STCs.

After considering the uncertainty scheme, there were STCs including

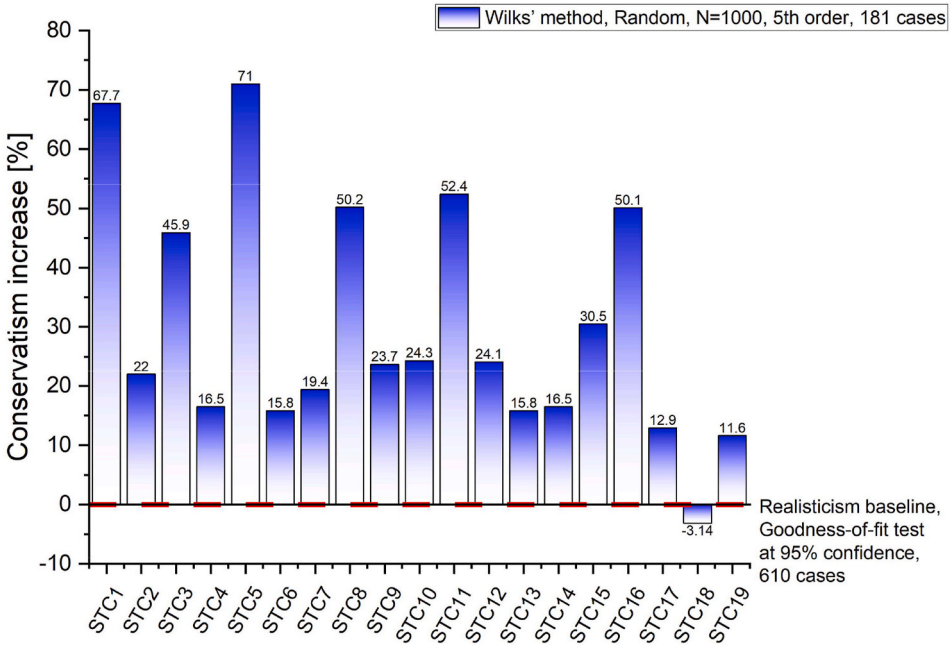

Fig. 17. Conservatism comparison of 95% confidential point of Cs-137 release between the 5th order of Wilks' method from the randomness cases at 1000 times and the goodness-of-fit test.

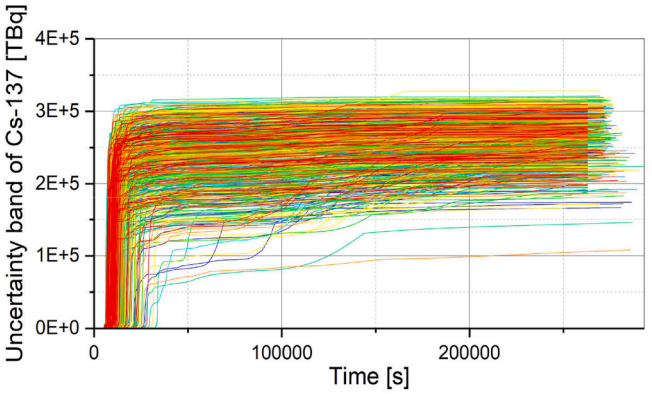

Fig. 18. Uncertainty band of Cs-137 release of STC18 [TBq].

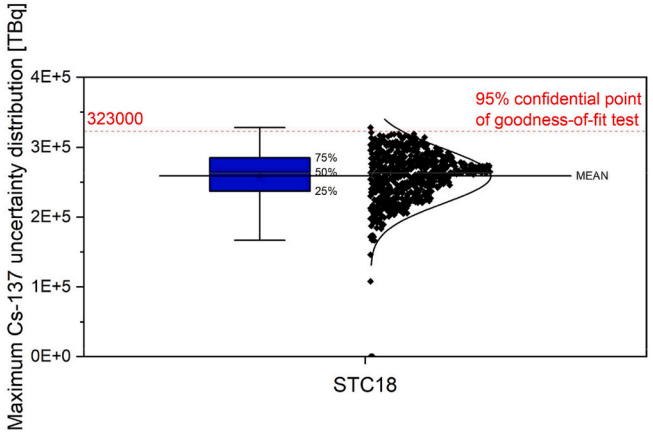

Fig. 19. Uncertainty distribution of Cs-137 release of STC18 [TBq].

STC3, STC5, and STC11 having Cs-137 releases less than 100 TBq from the conventional level 2 PSA provided the uncertainty propagation of Cs-137 releases exceeding 100 TBq. These three STC cases were able to provide the uncertainty increase of the Cs-137 release more than 10 times of 100 TBq. Thus, in the determination of risk safety goal, the Cs-137 consequences higher 100 TBq would be more considered for the possible consequences to people and the environment.

As for the 95% confidential point estimation of the Cs-137 release of parametric uncertainty analysis, all 19 STCs of the parametric uncertainty analysis provided consistent results whereby the 95% confidential points of empirical analysis had higher values than the goodness-of-fit test method harmonizingly their normal distribution assumption theory. The conservatism comparison of the parametric uncertainty analysis at 95% confidential point of Cs-137 release of all 19 STCs showed that the value of the goodness-of-fit test had the potential to represent the highest realistic point for the parametric method while that of empirical analysis could be recognized as the highest conservative point for the parametric method. Regarding non-parametric uncertainty analysis, the high randomness of Wilk's method at 1000 times helped confirm the 95% confidential point. The 1st order of Wilks' method (considering 59 cases) could represent the highest conservative case supporting safety regulation issues well while the 5th order of Wilks' method (considering 181 cases) would be able to express the realistic estimation of severing economic concerns. According to the investigation of the conservatism comparison between parametric and non-parametric uncertainty analysis methods, the parametric uncertainty analysis provided more realistic concerns than the non-parametric uncertainty analysis significantly.

Sensitivity analysis of 58 uncertainty parameters using Pearson correlation coefficient and Spearman correlation coefficient revealed seven dominant uncertainty parameters affecting Cs-137 release including 1st break area in the primary system, 2nd break area in the primary system, 1st break area of the steam generator tube, the Chi shape factor for non-spherical shapes of the aerosols, the number of operational low-pressure injection pumps, number of operating spray pumps for the upper part, and time period before early containment failure.

In summary, the development of the systematic framework to quantify realistic and conservative concerns of radioactive material

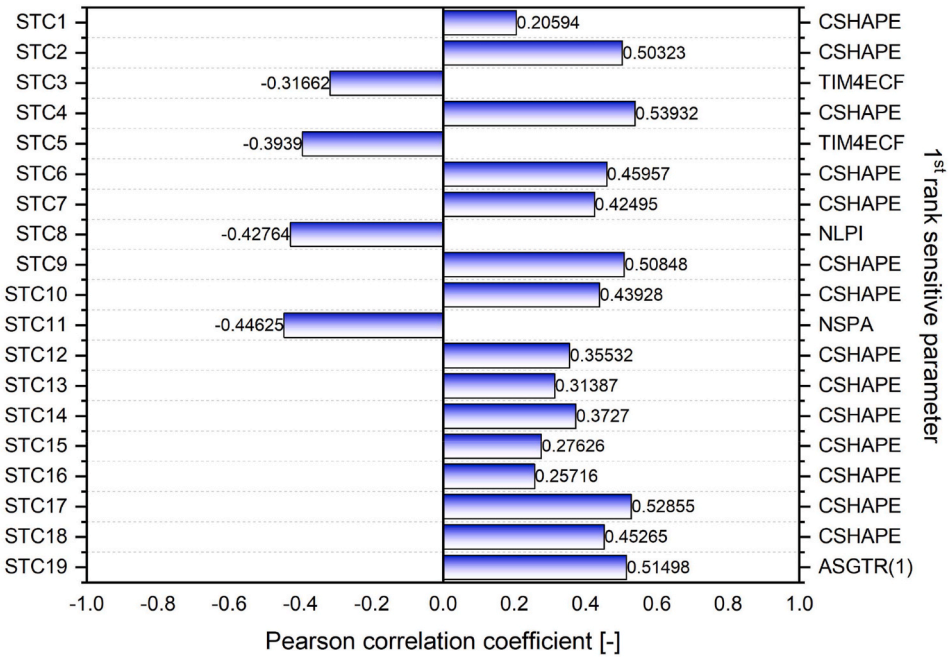

Fig. 20. 1st rank of uncertainty parameters affecting the Cs-137 release of all 19 STCs using Pearson correlation coefficient. (Hereafter uncertainty parameters would refer to the phenomena in Table 2).

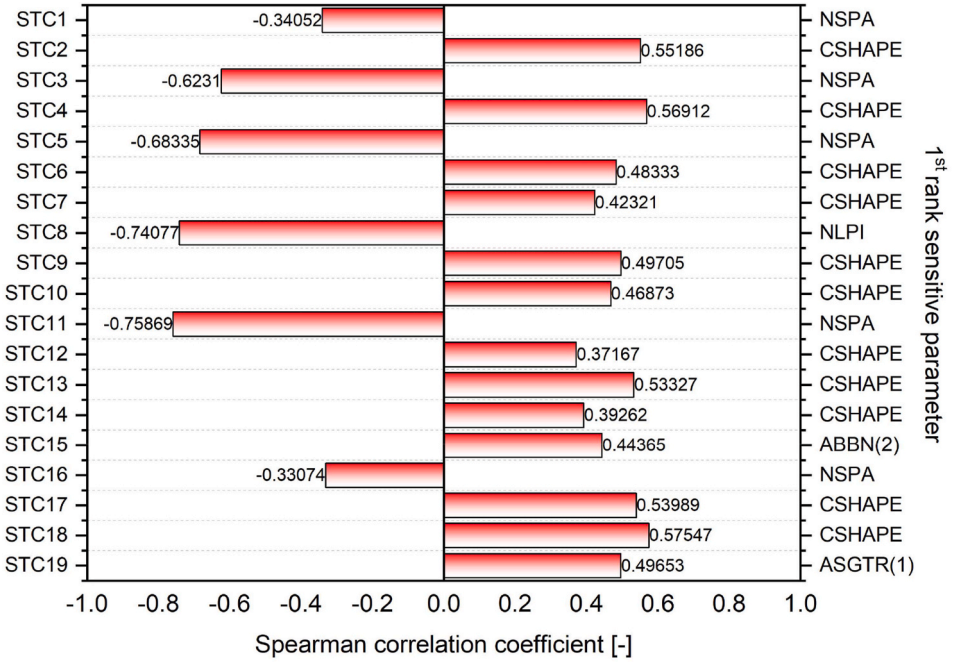

Fig. 21. 1st rank of uncertainty parameters affecting the Cs-137 release of all 19 STCs using Spearman correlation coefficient. (Hereafter uncertainty parameters would refer to the phenomena in Table 2).

release with sensitivity and uncertainty analysis using both parametric and non-parametric methods identified the understanding of the Cs-137 release characteristic covering realistic and conservative point estimations. This useful systematic framework is expected to be applied to other NPPs to properly and reasonably support safe and economic considerations in the future.

Declaration of competing interest

The authors declare that they have no known competing financial interests or personal relationships that could have appeared to influence the work reported in this paper.

Acknowledgments

This research was supported by the Chung-Ang University Research Grants in 2023. This work is also supported by the National Research Foundation of Korea (NRF) grant funded by the Korean government (MSIT: Ministry of Science and ICT) (No. RS-2022-00143695). Additionally, the authors must thank the opportunity from Korea Atomic

Energy Research Institute (KAERI) assnd Korea National University of Science and Technology (UST) for all facility and time resources in research period.

References

[1] International Atomic Energy Agency, Risk Management: A Tool for Improving Nuclear Power Plant Performance, IAEA, Vienna, Austria, 2001. IAEA-TECDOC-1209.

[2] S. Kaplan, B.J. Garrick, On the quantitative definition of risk, Risk Anal. 1 (1981) 1, https://doi.org/10.1111/j.1539-6924.1981.tb01350.x.

[3] S. Mahadevan, S. Sarkar, Uncertainty Analysis Methods, CBP-TR-2009-002, Rev. 0, IAEA, Austria, 2009.

[4] International Atomic Energy Agency, Applications of Probabilistic Safety Assessment (PSA) for Nuclear Power Plants, IAEA, Vienna, Austria, 2001. IAEA-TECDOC-1200.

[5] International Atomic Energy Agency, Nuclear Power Reactors in the World, IAEA-RDS-2/42, IAEA, Vienna, Austria, 2022.

[6] D.G. Kang, S.H. Ahn, Reevaluation of station blackout risk of OPR-1000 nuclear power plant applying combined approach of deterministic and probabilistic method, in: Proceedings of the 16th International Topical Meeting on Nuclear Reactor Thermal Hydraulics (NURETH-16), 2015. Chicago, IL, August 30 - September 4.

[7] T.J. Kim, Y.J. Cho, H.G. Lim, G.C. Park, Thermal hydraulic analysis for accidents in OPR1000 and evaluation of uncertainty for PSA, in: Proceedings of 20th International Conference on Structural Mechanics in Reactor Technology (SMiRT 20), 2009. Espoo, Finland, August 9-14.

[8] D.S. Kim, J.H. Park, H.G. Lim, A pragmatic approach to modeling common cause failures in multi-unit PSA for nuclear power plant sites with a large number of units, Reliab Eng Syst 195 (2020) 106739, https://doi.org/10.1016/j.ress.2019.106739.

[9] J.H. Cho, S.H. Han, D.S. Kim, H.G. Lim, Multi-unit level 2 probabilistic safety assessment: approaches and their application to a six-unit nuclear power plant site, Nucl. Eng. Technol. 50 (2018) 8, https://doi.org/10.1016/j.net.2018.04.005.

[10] J.H. Cho, S.H. Lee, Y.S. Bang, S.W. Lee, S.Y. Park, Exhaustive simulation approach for severe accident risk in nuclear power plants: OPR-1000 full-power internal events, Reliab Eng Syst 225 (2022) 108580, https://doi.org/10.1016/j.ress.2022.108580.

[11] S.Y. Kim, K.H. Lee, S.Y. Park, S.J. Han, K.I. Ahn, S.W. Hwang, Interfacing between MAAP and MACCS to perform radiological consequence analysis, Nucl. Eng. Technol. 54 (2022) 4, https://doi.org/10.1016/j.net.2021.10.001.

[12] International Atomic Energy Agency, Defence in Depth in Nuclear Safety, A Report by the International Nuclear Safety Advisory Group (INSAG), IAEA, Vienna, Austria, 1996. INSAG-10.

[13] K. Silva, K. Okamoto, Discussion on probability of cesium-137 release exceeding 100 TBq as a part of the consideration of nuclear power plant probabilistic risk criteria for environmental protection, Reliab Eng Syst 180 (2018) 88–93, https://doi.org/10.1016/j.ress.2018.07.013.

[14] X. Zheng, H. Itoh, H. Tamaki, Y. Maruyama, An integrated approach to source term uncertainty and sensitivity analyses for nuclear reactor severe accidents, J. Nucl. Sci. Technol. 53 (2016) 3, https://doi.org/10.1080/00223131.2015.1044262.

[15] X. Shi, J. Sun, Q. Chen, H. Wang, Uncertainty analysis and its application of radioactive source term of HPR1000 under severe accident, Int J Adv Nucl Reactor Des Technol 3 (2021) 134–138, https://doi.org/10.1016/j.jandt.2021.07.004.

[16] H. Park, M. Jae, Uncertainty analysis of source term and off-site consequence for WH600 using MELCOR and WinMACCS, Ann. Nucl. Energy 175 (2022) 109175, https://doi.org/10.1016/j.anucene.2022.109175.

[17] F.D. Auria, Best estimate plus uncertainty (BEPU): status and perspectives, Nucl. Eng. Des. 352 (2019) 110190, https://doi.org/10.1016/j.nucengdes.2019.110190.

[18] Fauske & Associates LLC (FAI), Modular Accident Analysis Program 5.05 (MAAP5.05), Electric Power Research Institute, Washington, DC, 2019.

[19] J.D. Sheskin, Handbook of Parametric and Nonparametric Statistical Procedures, second ed., Chapman& Hall/CRC, Boca Raton, FL, 2000.

[20] H.G. Lim, S.H. Han, J.J. Jeong, Mosaique – a network based software for probabilistic uncertainty analysis of computerized simulation models, Nucl. Eng. Des. 241 (2011) 5, https://doi.org/10.1016/j.nucengdes.2011.01.021.

[21] International Atomic Energy Agency, Best Estimate Safety Analysis for Nuclear Power Plants: Uncertainty Evaluation, IAEA, Vienna, Austria, 2008. Safety reports series No.52, STI/PUB/1306.

[22] S. Han, T.W. Kim, Numerical experiments on order statistics method based on Wilks' formula for best-estimate plus uncertainty methodology, J. Environ. Manag. 235 (2019) 28–33, https://doi.org/10.1016/j.jenvman.2019.01.050.

[23] J.D. Chee, Pearson's Product-Moment Correlation: Sample Analysis, University of Hawaii at Manoa School of Nursing, Honolulu, HI, 2015.

[24] Centre for Innovation in Mathematics Teaching. Statistics, Chapter 12 Correlation and Regression, Ingram Publisher Services UK, Plymouth, UK, 2000.

[25] A.A.K. Alhameeda, Spearman's correlation coefficient in statistical analysis, Int. J. Nonlinear Anal. Appl. 13 (2022) 1, https://doi.org/10.22075/ijnaa.2022.6079.

[26] Mathematics Education Centre, Statstutor, Spearman's Correlation. Loughborough, Loughborough University, UK, 2004.

[27] R. Sturm, Theoretical models for dynamic shape factors and lung deposition of small particle aggregates originating from combustion processes, Z. Med. Phys. 20 (2010) 3, https://doi.org/10.1016/j.zemedi.2010.04.001.